Functional Role of High-Affinity Anandamide Transport, as Revealed by Selective Inhibition

M. Beltramo, N. Stella, A. Calignano, S. Y. Lin, A. Makriyannis, D. Piomelli*

Anandamide, an endogenous ligand for central cannabinoid receptors, is released from neurons on depolarization and rapidly inactivated. Anandamide inactivation is not completely understood, but it may occur by transport into cells or by enzymatic hydrolysis. The compound *N*-(4-hydroxyphenyl)arachidonylamide (AM404) was shown to inhibit high-affinity anandamide accumulation in rat neurons and astrocytes in vitro, an indication that this accumulation resulted from carrier-mediated transport. Although AM404 did not activate cannabinoid receptors or inhibit anandamide hydrolysis, it enhanced receptor-mediated anandamide responses in vitro and in vivo. The data indicate that carrier-mediated transport may be essential for termination of the biological effects of anandamide, and may represent a potential drug target.

Anandamide (arachidonylethanolamide) is an endogenous lipid that activates brain cannabinoid receptors and mimics the pharmacological effects of Δ^9-tetrahydrocannabinol, the active principle of hashish and marijuana (*1*). In humans, such effects include euphoria, calmness, dream states, and drowsiness (*2*). Depolarized neurons release anandamide (*3*) through a mechanism that may require the calcium-dependent cleavage of a phospholipid precursor in neuronal membranes (*4*). Like other modulatory substances, extracellular anandamide is thought to be rapidly inactivated, but the exact nature of this inactivating process is still unclear. A possible pathway is hydrolysis to arachidonic acid and ethanolamine, catalyzed by a membrane-bound fatty acid amide hydrolase (FAAH) highly expressed in rat brain and liver (*5*). Nevertheless, the low FAAH activity found in brain plasma membranes indicates that this enzyme may be intracellular (*5*), a possibility that is further supported by sequence analysis of rat FAAH (*6*). Although anandamide could gain access to FAAH by passive diffusion, the transfer rate is expected to be low because of the molecular size of this lipid mediator (*7*). In that other lipids including polyunsaturated fatty acids and prostaglandin E_2 (PGE_2) enter cells by carrier-mediated transport (*8, 9*), it is possible that anandamide uses a similar mechanism. Indeed, the existence of a rapid, saturable process of anandamide accumulation into neural cells has been reported (*3*). This accumulation may result from the activity of a transmembrane carrier, which may thus participate in termination of the biological actions of anandamide. Accordingly, we developed drug inhibitors of anandamide transport and investigated their pharmacological properties in cultures of rat cortical neurons or astrocytes.

The accumulation of exogenous [^{3}H]anandamide by neurons or astrocytes fulfills several criteria of a carrier-mediated transport (Fig. 1) (*10*). It is a rapid process that reaches 50% of its maximum within about 4 min (Fig. 1A). Furthermore, [^{3}H]anandamide accumulation is temperature-dependent (Fig. 1A) and saturable (Fig. 1, B and C). Kinetic analyses revealed that accumulation in neurons can be represented by two components of differing affinities (lower affinity: Michaelis constant, K_m, = 1.2 μM, maximum accumulation rate, V_{max}, = 90.9 pmol/min per milligram of protein; higher affinity: K_m = 0.032 μM, V_{max} = 5.9 pmol/min per milligram of protein) (Fig. 1B). The higher affinity component may reflect a binding site, however, as it is displaced by the cannabinoid receptor antagonist, SR-141716-A (100 nM) (*11*). In astrocytes, [^{3}H]anandamide accumulation is represented by a single high-affinity component (K_m = 0.32 μM, V_{max} = 171 pmol/min per milligram of protein) (Fig. 1C). Such apparent K_m values are similar to those of known neurotransmitter uptake systems (*12*) and are suggestive therefore of high-affinity carrier-mediated transport.

To characterize further this putative anandamide transport, we used cortical astrocytes in culture. As expected from a selective process, the temperature-sensitive component of [^{3}H]anandamide accumulation was prevented by nonradioactive anandamide, but not by palmitoylethanolamide, arachidonate, prostanoids, or leukotrienes (Fig. 2A). Replacement of extracellular Na^+ with *N*-dimethylglucosamine or choline had no effect (as percentage of control: *N*-dimethylglucosamine, 124 ± 12%; choline, 98 ± 14%; mean ± SEM, n = 6), suggesting that [^{3}H]anandamide accumulation is mediated by a Na^+-independent mechanism, which has been observed with other lipids (*8, 9*). Moreover, inhibition of FAAH activity by treating the cells with (*E*)-6-(bromomethylene)tetrahydro-3-(1-naphthalenyl)-2*H*-pyran-2-one (25 μM) or linoleyl trifluoromethyl ketone (15 μM) (*13, 14*) had no effect (Fig. 2, B and C). This indicates that anandamide hydrolysis did not provide the driving force for anandamide transport into astrocytes within the

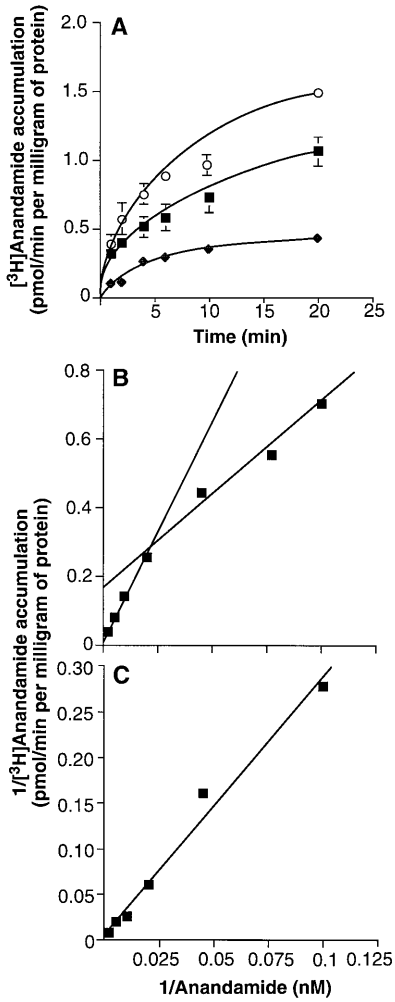

Fig. 1. (**A**) Time course of [^{3}H]anandamide accumulation in rat cortical neurons (circles) or astrocytes (squares) at 37°C, and astrocytes at 0° to 4°C (diamonds). Results are expressed as mean ± SEM of 6 to 12 independent determinations. (**B** and **C**) Lineweaver-Burk analyses of [^{3}H]anandamide accumulation (37°C, 4 min) in neurons (B) or astrocytes (C). Results are from one experiment representative of three performed in duplicate with each cell type. The [^{3}H]anandamide accumulation assay has been described (*10*).

M. Beltramo, N. Stella, D. Piomelli, The Neurosciences Institute, 10640 J. J. Hopkins Drive, San Diego, CA 92121, USA.
A. Calignano, School of Pharmacy, University of Naples, Italy 80131.
S. Y. Lin and A. Makriyannis, School of Pharmacy, University of Connecticut, Storrs, CT 06269, USA.
*To whom correspondence should be addressed. E-mail: piomelli@nsi.edu

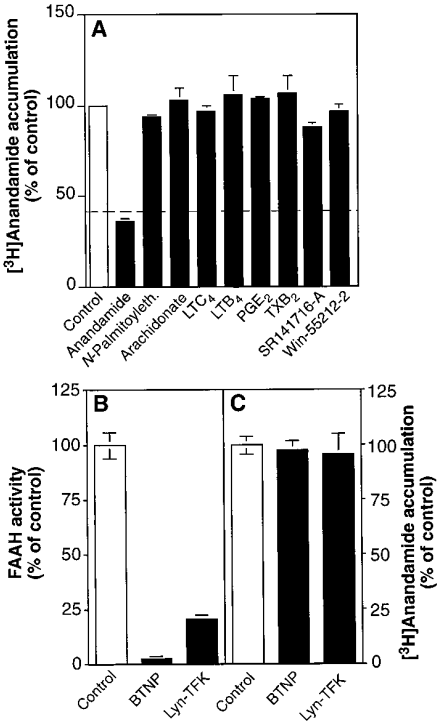

Fig. 2. (**A**) Selectivity of [^{3}H]anandamide accumulation in cortical astrocytes. Accumulation was measured after a 4-min incubation with [^{3}H]anandamide at 37°C, in the absence (control) or presence of nonradioactive anandamide (100 μM), *N*-palmitoylethanolamide (100 μM), arachidonate (100 μM), leukotriene C_4 (LTC_4; 1 μM), leukotriene B_4 (LTB_4; 1 μM), PGE_2 (100 μM), or thromboxane B_2 (TXB_2; 50 μM). The broken line indicates nonspecific [^{3}H]anandamide accumulation in cells measured at 0° to 4°C (43 ± 3% of total accumulation, which in these experiments was 43,104 ± 1249 dpm per well). Results are expressed as mean ± SEM (n = 6 to 9). Effects of FAAH inhibitors on (**B**) FAAH activity and (**C**) [^{3}H]anandamide accumulation in cortical astrocytes. Cells were incubated for 10 min with (*E*)-6-(bromomethylene)tetrahydro-3-(1-naphthalenyl)-2*H*-pyran-2-one (BTNP, 25 μM) or linoleyl trifluoro methylketone (Lyn-TFK, 15 μM), and then with the same drugs plus [^{3}H]anandamide for an additional 20 min. The total radioactivity in cell lipid extracts (to measure [^{3}H]anandamide transport) (*10*) and radioactivity in nonesterified arachidonate (to measure FAAH activity) (*13*) were measured separately in samples of lipid extracts prepared from the same cultures.

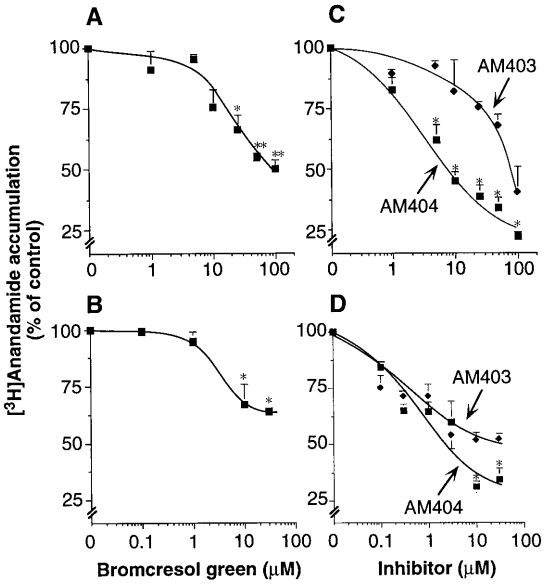

Fig. 3. Inhibition of [^{3}H]anandamide accumulation by bromcresol green in (**A**) astrocytes or (**B**) neurons. One asterisk indicates $P < 0.05$ and two asterisks $P < 0.01$ [analysis of variance (ANOVA) followed by Bonferroni test] compared with control [^{3}H]anandamide accumulation. Inhibition of [^{3}H]-anandamide accumulation by AM404 (squares) or AM403 (diamonds) in (**C**) astrocytes or (**D**) neurons. The asterisk indicates $P < 0.05$ (paired Student's t test between AM404 and AM403). In all experiments, cells were incubated with the inhibitors for 10 min before the addition of [^{3}H]anandamide for an additional 4 min. Results are expressed as mean ± SEM of three to nine independent determinations.

time frame of our experiments. Finally, the cannabinoid receptor agonist WIN-55212-2 (1 μM) and antagonist SR-141716-A (10 μM) also had no effect, suggesting that receptor internalization was not involved (Fig. 2A).

A primary criterion for defining carrier-mediated transport is pharmacological inhibition. To identify inhibitors of anandamide transport, we first examined compounds that prevent the cellular uptake of other lipids, such as fatty acids (phloretin, 50 μM), phospholipids (verapamil, 100 μM; quinidine, 50 μM), or PGE_2 (bromcresol green, 0.1 to 100 μM) (*15*). Among the compounds tested, only bromcresol green interfered with anandamide transport, albeit with limited potency and partial efficacy (Fig. 3, A and B). Bromcresol green inhibited [^{3}H]anandamide accumulation with an IC_{50} (concentration needed to produce half-maximal inhibition) of 4 μM in neurons and 12 μM in astrocytes and acted noncompetitively (*16*). Moreover, bromcresol green had no significant effect on the binding of [^{3}H]WIN-55212-2 to rat cerebellar membranes (inhibition constant, K_i, = 22 μM), FAAH activity in rat brain microsomes (IC_{50} > 50 μM), and uptake of [^{3}H]arachidonate or [^{3}H]ethanolamine in astrocytes (121 ± 13% and 103 ± 12%, respectively, at 50 μM bromcresol green, n = 3) (*17*). The sensitivity to bromcresol green, which blocks PGE_2 transport, raised the question of whether anandamide accumulation occurred by means of a PGE_2 carrier. That this is not the case was shown by the lack of [^{3}H]PGE_2 accumulation in neurons or astrocytes (*18*) and by the inability of PGE_2 to interfere with [^{3}H]anandamide accumulation (Fig. 2A). Previous results indicating that expression of PGE_2 transporter mRNA in brain tissue is not detectable further support this conclusion (*9*).

To search for more potent anandamide transport inhibitors, we synthesized and tested a series of structural analogs of anandamide (*19*). From this screening, we selected the compound *N*-(4-hydroxyphenyl)arachidonylamide (AM404), which was both efficacious and relatively potent (Fig. 3, C and D; IC_{50} was 1 μM in neurons and 5 μM in astrocytes). As we anticipated from its chemical structure, AM404 acted as a competitive inhibitor (*20*), suggesting that it may serve as a transport substrate or pseudosubstrate. In contrast, at the concentrations tested AM404 had no effect on FAAH activity (IC_{50} > 30 μM) or on uptake of [^{3}H]arachidonate or [^{3}H]ethanolamine (102 ± 4% and 96 ± 14%, respectively, at 20 μM AM404, n = 6). Furthermore, a positional isomer of AM404, *N*-(3-hydroxyphenyl)-arachidonylamide (AM403), was significantly less effective than AM404 in inhibiting transport (Fig. 3, C and D). These data provide pharmacological evidence for the existence of a specific anandamide transporter and suggest (i) that neurons and astrocytes may act synergistically in the brain to dispose of extracellular anandamide and (ii) that the transport systems in these two cell types may differ kinetically and pharmacologically (Fig. 1, B and C, and Fig. 3, C and D).

The identification of inhibitors allowed us to examine whether transmembrane transport participates in terminating anandamide responses mediated by cannabinoid receptor activation. Cannabinoid receptors of the CB1 subtype are expressed in neurons (*21*) where they are negatively coupled to adenylyl cyclase activity (*22*). Accordingly, in cultures of rat cortical neurons the cannabinoid receptor agonist WIN-55212-2 inhibited forskolin-stimulated adenosine 3′,5′-monophosphate (cAMP) accumulation (control: 39 ± 4 pmol per milligram of protein; 3 μM forskolin: 568 ± 4 pmol per milligram of protein; forskolin plus 1 μM WIN-55212-2: 220 ± 24 pmol per milligram of protein), and this inhibition was prevented by the antagonist SR-141716-A (1 μM) (555 ± 39 pmol/mg of protein, n = 9) (*23*). Anandamide produced a similar effect, but with a potency (IC_{50}, 1 μM) that was 1/20 of that expected from its binding

constant for CB1 cannabinoid receptors ($K_i \approx 50$ nM) (*1*) (Fig. 4A). The transport inhibitor AM404 bound to CB1 receptors with low affinity ($K_i = 1.8$ μM) (*19*) and did not reduce cAMP concentrations when applied at 10 μM (Fig. 4B). Nevertheless, the drug enhanced the effects of anandamide, increasing the potency (by a factor of 10) and decreasing the threshold (by a factor of 1/100), an effect that was prevented by SR-141716-A (Fig. 4A). Thus, a concentration of anandamide that was below threshold when applied alone (0.3 μM) produced an almost maximal effect when applied with AM404 (Fig. 4B). Bromcresol green and AM403, which were less effective than AM404 in inhibiting anandamide transport (Fig. 3), were also less effective in enhancing the anandamide response (Fig. 4B). Furthermore, the decreases in cAMP concentrations produced by WIN-55212-2 (which stimulates CB1 receptors but is not subject to physiological clearance) or glutamate [which stimulates metabotropic receptors negatively coupled to adenylyl cyclase (*24*) and is cleared by a selective transporter (*25*)] are not affected by any of the anandamide transport inhibitors tested (*26*).

These results suggest that pharmacological blockade of carrier-mediated transport protects anandamide from physiological inactivation, enhancing the potency of anandamide to nearly that expected from its affinity for CB1 cannabinoid receptors in vitro. To find out whether this potentiation occurs in vivo, we tested the effects of AM404 on the antinociceptive activity of anandamide in mice. Intravenous anandamide (20 mg per kilogram of body weight) elicited a modest but significant analgesia, as measured by the hot plate test (*27*) ($P < 0.05$, Student's t test); this analgesia disappeared 60 min after injection and was prevented by SR-141716-A (Fig. 4C) (*28*). Administration of AM404 (10 mg/kg, intravenously) had no antinociceptive effect within 60 min of injection but significantly enhanced and prolonged anandamide-induced analgesia (Fig. 4C) ($P < 0.01$, Student's t test).

Our findings indicate that a high-affinity transport system present in neurons and astrocytes has a role in anandamide inactivation by removing this lipid mediator from the extracellular space and delivering it to intracellular metabolizing enzymes such as FAAH (*5*, *6*). Therefore, the identification of selective inhibitors of anandamide transport should be instrumental in understanding the physiological roles of the endogenous cannabinoid system and may lead to the development of therapeutic agents.

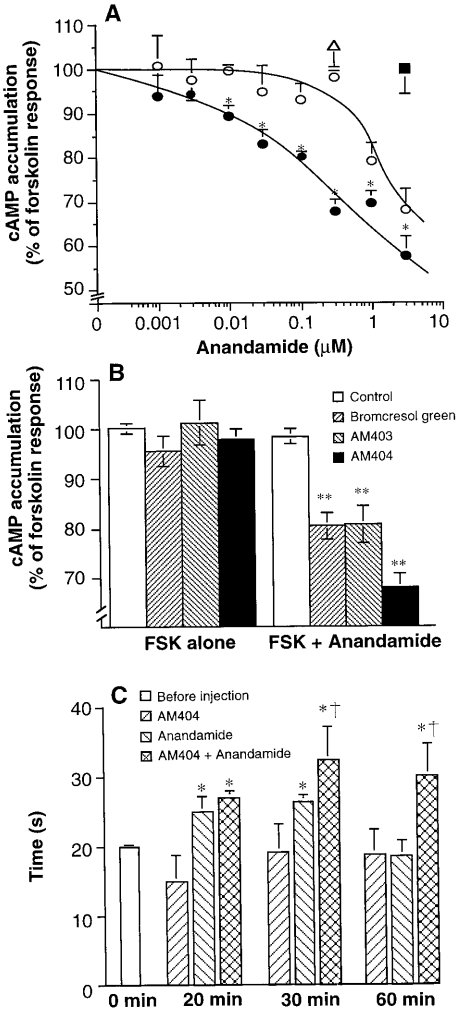

Fig. 4. (**A**) Effects of AM404 on anandamide-induced inhibition of adenylyl cyclase activity in cortical neurons. The neurons were stimulated with forskolin (3 μM) in the presence of anandamide (0.001 to 3 μM; open circles), anandamide (0.001 to 3 μM) plus AM404 (10 μM) (filled circles), anandamide (3 μM) plus SR-141716-A (1 μM) (square), or anandamide (0.3 μM) plus AM404 (10 μM) and SR-141716-A (1 μM) (triangle). (**B**) Effects of anandamide transport inhibitors on anandamide-induced inhibition of adenylyl cyclase activity. Forskolin (FSK)-stimulated neurons were incubated with AM404, AM403, or bromcresol green (each at 10 μM) without (FSK alone) or with (FSK + anandamide) 0.3 μM anandamide. Results are expressed as mean ± SEM of nine independent determinations. One asterisk indicates $P < 0.05$ and two asterisks $P < 0.01$ (ANOVA followed by Bonferroni test). (**C**) Effects of AM404 on the analgesic activity of anandamide in the hot plate test. Three groups of six mice received AM404 (10 mg/kg, intravenous), anandamide (20 mg/kg, intravenous), or anandamide plus AM404. The hot plate test (55.5°C) was performed at the times indicated, and latency to jump (in seconds) was measured before (control) and after the drugs were injected. In all groups, latency to jump before injections was 21 ± 0.6 s ($n = 18$). A fourth group of mice received injections of vehicle alone (saline containing 20% dimethyl sulfoxide), which did not affect latency to jump. One asterisk indicates $P < 0.05$ compared with uninjected controls (ANOVA followed by Bonferroni test), and one cross indicates $P < 0.01$ compared with anandamide-treated animals (Student's t test).

REFERENCES AND NOTES

1. W. A. Devane *et al*., *Science* **258**, 1946 (1992); R. Mechoulam, L. Hanuš, B. R. Martin, *Biochem. Pharmacol.* **48**, 1537 (1994).
2. W. L. Dewey, *Pharmacol. Rev.* **38**, 151 (1986).
3. V. Di Marzo *et al*., *Nature* **372**, 686 (1994).
4. H. Cadas, S. Gaillet, M. Beltramo, L. Venance, D. Piomelli, *J. Neurosci.* **16**, 3934 (1996); T. Sugiura *et al*., *Eur. J. Biochem.* **240**, 53 (1996); H. Cadas, E. di Tomaso, D. Piomelli, *J. Neurosci*., **17**, 1226 (1997).
5. D. G. Deutsch and S. Chin, *Biochem. Pharmacol.* **46**, 791 (1993); F. Desarnaud, H. Cadas, D. Piomelli, *J. Biol. Chem.* **270**, 6030 (1995); N. Ueda, Y. Kurahashi, S. Yamamoto, T. Tokunaga, *ibid*., p. 23823.
6. B. Cravatt *et al*., *Nature* **384**, 83 (1996).
7. W. D. Stein, *Channels and Pumps. An Introduction to Membrane Transport*, (Academic Press, San Diego, 1990), pp. 53–57.
8. L. Z. Bito, *Nature* **256**, 1234 (1975); J. E. Schaffer and H. F. Lodish, *Cell* **79**, 427 (1994); I. N. Bojesen and E. Bojesen, *Acta Physiol. Scand.* **156**, 501 (1996).
9. N. Kanai *et al*., *Science* **268**, 866 (1995).
10. Cultures of cortical neurons [N. Stella, L. Pellerin, P. Magistretti, *J. Neurosci.* **15**, 3307 (1995)] or astrocytes (*13*) were prepared from rat embryos and were used after 4 to 6 days and 21 to 25 days in vitro, respectively. Accumulation of [^{3}H]anandamide (221 Ci/mmol, New England Nuclear, Wilmington, DE) was measured by incubating the cells (six-well plates) for various times in Krebs buffer [136 mM NaCl, 5 mM KCl, 1.2 mM $MgCl_2$, 2.5 mM $CaCl_2$, 10 mM glucose, and 20 mM Trizma base; (pH 7.4), at 37°C] containing [^{3}H]anandamide (0.45 nM, brought to 100 nM with nonradioactive anandamide). Incubations were stopped by aspirating the media, and cells were rinsed with Krebs buffer containing bovine serum albumin (BSA, 0.1% w/v) and subjected to extraction with methanol and chloroform. Radioactivity in the extracts was measured directly or after fractionation of cell lipids by thin-layer chromatography (*13*). For kinetic analyses, the neurons were incubated for 4 min at 37°C in the presence of 10 to 500 nM anandamide containing 0.05 to 2.5 nM [^{3}H]anandamide. We subtracted nonspecific accumulation (measured at 0° to 4°C) before determining kinetic constants by Lineweaver-Burk analysis.
11. M. Beltramo and D. Piomelli, unpublished data.
12. E. L. Barker and R. D. Blakely, in *Psychopharmacology: The Fourth Generation of Progress*, F. E. Bloom and D. J. Kupfer, Eds. (Raven, New York, 1995), pp. 321–334. In a previous study with mixed cultures of rat cortical neurons and astrocytes, a K_m of 30 μM for [^{3}H]anandamide accumulation was obtained (*3*). Such a high value likely resulted from the low specific radioactivity (0.3 mCi/mmol) of the [^{3}H]anandamide used.
13. M. Beltramo, E. di Tomaso, D. Piomelli, *FEBS Lett.* **403**, 263 (1997).
14. B. Koutek *et al*., *J. Biol. Chem.* **269**, 22937 (1994).
15. L. Z. Bito, H. Davson, E. V. Salvador, *J. Physiol.* **256**, 257 (1976); W. Stremmel and P. D. Berk, *Proc. Natl. Acad. Sci. U.S.A.* **83**, 3086 (1986); S. Ruetz and P. Gros, *Cell* **77**, 1071 (1994).
16. In astrocytes, V_{max} values for [^{3}H]anandamide accumulation were 200 pmol/min per milligram of protein without bromcresol green, and 111 pmol/min per milligram of protein with bromcresol green (10 μM). Apparent K_m values were 0.24 and 0.25 μM, respectively ($n = 6$).
17. Displacement of [^{3}H]WIN-55212-2 binding (40 to 60 Ci/mmol; New England Nuclear) to rat cerebellar

membranes (0.1 mg/ml) was determined as described [J. E. Kuster *et al*., *J. Pharmacol. Exp. Ther.* **264**, 1352 (1993)]. Nonspecific binding was measured in the presence of 1 μM nonradioactive WIN-55212-2. FAAH activity was measured in rat brain particulate fractions as described (*13*). The uptake of [^{3}H]arachidonate (Amersham, 200 Ci/mmol; 5 nM brought to 100 nM) and [^{3}H]ethanolamine (Amersham, 50 Ci/mmol; 20 nM brought to 100 nM) was determined on cortical astrocytes for 4 min as described (*10*). The control uptake for [^{3}H]arachidonate was 16729 ± 817 dpm per well and for [^{3}H]ethanolamine it was 644 ± 100 dpm per well (n = 6).

18. Neurons or astrocytes were incubated for 4 min at 37°C in Krebs buffer containing [^{3}H]PGE_2 (0.67 nM brought to 100 nM with nonradioactive PGE_2; 171 Ci/mmol, New England Nuclear). After rinsing with Krebs buffer containing BSA, we subjected the cells to lipid extraction and counted radioactivity in the extracts. On average, neurons contained 245 ± 65 dpm per well and astrocytes 302 ± 20 dpm per well; nonspecific accumulation in astrocytes at 0° to 4°C was 355 ± 28 dpm per well (n = 6).
19. A. Khanolkar *et al*., *J. Med. Chem.* **39**, 4515 (1996).
20. In astrocytes, apparent K_m values for [^{3}H]anandamide accumulation were 0.11 μM without AM404 and 0.27 μM with AM404 (10 μM). V_{max} values were 29 pmol/min per milligram of protein without AM404 and 26 pmol/min per milligram of protein with AM404, respectively (n = 6).
21. M. Herkenham *et al*., *Proc. Natl. Acad. Sci. U.S.A.* **87**, 1932 (1990); L. A. Matsuda, T. I. Bonner, S. J. Lolait, *J. Comp. Neurol.* **327**, 535 (1993).
22. A. C. Howlett, J. M. Qualy, L. L. Khachatran, *Mol. Pharmacol.* **29**, 307 (1986); M. Jung *et al*., *J. Neurochem.* **68**, 402 (1997).
23. Cortical neurons were prepared in 12-well plates and used after 4 to 6 days in vitro. Incubations were carried out in the presence of forskolin (3 μM) and isobutyl methyl xanthine (1 mM). The cAMP concentrations were measured by radioimmunoassay with a commercial kit (Amersham, Arlington, IL) and following manufacturer's instructions.
24. L. Prézeau *et al*., *Proc. Natl. Acad. Sci. U.S.A.* **89**, 8040 (1992).
25. R. Maki, M. B. Robinson, M. A. Dichter, *J. Neurosci.* **14**, 6754 (1994).
26. The amounts of cAMP in the presence of a concentration of WIN-55212-2 below threshold (1 nM, determined in preliminary experiments) were 96.7 ± 2.5% of forskolin alone and were not significantly affected by 10 μM AM404 (89.8 ± 2.6%), 10 μM AM403 (92.4 ± 2.3%), or 10 μM bromcresol green (92.9 ± 2.3%) (n = 3). In the presence of a concentration of glutamate below threshold (3 μM) (*24*), cAMP concentrations were 91.6 ± 2% of forskolin alone and were not significantly affected by AM404 (84.4 ± 4.9%), AM403 (89.5 ± 2.4%), or bromcresol green (84.4 ± 3%) (n = 3).
27. E. Fride and R. Mechoulam, *Eur. J. Pharmacol.* **231**, 313 (1993); P. B. Smith *et al*., *J. Pharmacol. Exp. Ther.* **270**, 219 (1994).
28. The hot plate test (55.5°C) was carried out on male Swiss mice (25 to 30 g, Nossan, Italy) following standard procedures [F. Porreca, H. L. Mosberg, R. Hurst, V. J. Hruby, T. F. Burks, *J. Pharmacol. Exp. Ther.* **230**, 341 (1994)]. Anandamide and AM404 were dissolved in 0.9% NaCl solution containing 20% dimethyl sulfoxide and injected intravenously at 20 mg/kg and 10 mg/kg, respectively. To determine whether cannabinoid receptors participate in the effect of anandamide, we administered anandamide (20 mg/kg intravenously) or anandamide plus SR141716-A (2 mg/kg, subcutaneously) to two groups of six mice each. In mice that received anandamide alone, latency to jump increased from 21.7 ± 1.5 s to 30.7 ± 0.8 s ($P < 0.05$, ANOVA) 20 min after injection. In contrast, in mice that received anandamide plus SR141716-A, the latency to jump was not affected (19.6 ± 3.1 s).
29. We thank E. di Tomaso and H. Cadas for help and E. Barker, L. Parsons, and P. Schweitzer for critical reading of the manuscript. Supported by the Neuroscience Research Foundation, which receives major support from Novartis.

4 February 1997; accepted 17 June 1997

An NGF-TrkA–Mediated Retrograde Signal to Transcription Factor CREB in Sympathetic Neurons

Antonella Riccio,* Brian A. Pierchala,* Christopher L. Ciarallo, David D. Ginty†

Nerve growth factor (NGF) is a neurotrophic factor secreted by cells that are the targets of innervation of sympathetic and some sensory neurons. However, the mechanism by which the NGF signal is propagated from the axon terminal to the cell body, which can be more than 1 meter away, to influence biochemical events critical for growth and survival of neurons has remained unclear. An NGF-mediated signal transmitted from the terminals and distal axons of cultured rat sympathetic neurons to their nuclei regulated phosphorylation of the transcription factor CREB (cyclic adenosine monophosphate response element–binding protein). Internalization of NGF and its receptor tyrosine kinase TrkA, and their transport to the cell body, were required for transmission of this signal. The tyrosine kinase activity of TrkA was required to maintain it in an autophosphorylated state upon its arrival in the cell body and for propagation of the signal to CREB within neuronal nuclei. Thus, an NGF-TrkA complex is a messenger that delivers the NGF signal from axon terminals to cell bodies of sympathetic neurons.

The growth and survival of many populations of neurons depends on trophic support provided by their target tissue (*1*). NGF is secreted by targets of sympathetic and some sensory neurons, and it is also expressed within discrete regions of the central nervous system (*1*, *2*). NGF belongs to a family of structurally related neurotrophic factors termed neurotrophins; this family includes brain-derived neurotrophic factor (BDNF), neurotrophin 3 (NT-3), and neurotrophin 4/5 (NT-4/5) (*2*). Two cell surface receptors for NGF have been identified: a receptor tyrosine kinase, TrkA, and the low-affinity neurotrophin receptor, $p75^{NTR}$. NGF exerts its growth- and survival-promoting effects on neurons through activation of TrkA and subsequent biochemical events that ultimately influence the expression of various genes, including those encoding ion channels, neurotransmitter-synthesizing enzymes, and cytoskeletal components (*3*).

NGF stimulates dimerization and autophosphorylation of TrkA and initiation of intracellular signaling cascades that propagate the signal to the nucleus (*4*). One transcription factor that is a key target of an NGF-stimulated signaling pathway is CREB (*5*). Upon exposure of pheochromocytoma-derived cell line PC12 to NGF, CREB becomes phosphorylated on its transcriptional regulatory site Ser^{133} (*5*), and this phosphorylation event promotes NGF activation of transcription of the immediate early gene c-*fos*. Because many NGF-regulated immediate early genes and delayed-response genes contain CREB binding sites within their upstream regulatory regions (*5*), CREB is likely to be a mediator of the general nuclear response to neurotrophins.

Because NGF is internalized and retrogradely transported from the axon terminal to the cell body (*6*), NGF itself may carry signals from the axon terminal to the nucleus. Alternatively, TrkA or $p75^{NTR}$, an NGF-receptor complex, or a terminally derived second messenger molecule might serve as a retrograde messenger (*7*). To address questions of retrograde NGF signaling, we used compartmentalized cultures of sympathetic neurons (*8*) and antibodies that distinguish between the Ser^{133}-phosphorylated and unphosphorylated states of CREB (anti–P-CREB) (*9*) and TrkA (anti–P-Trk) (Fig. 1A). In these cultures, the cell bodies are separated from the axon terminals and distal processes by a distance of either 1 mm or 3 to 4 mm, and the cell bodies and distal processes are located in separate fluid compartments (Fig. 1B). This system enables us to expose isolated terminals and distal axonal processes to NGF and then to assess by immunocytochemistry the phosphorylation state of CREB Ser^{133} and TrkA in cell bodies.

To determine whether NGF induces phosphorylation of CREB Ser^{133} in sympa-

Department of Neuroscience, Johns Hopkins University School of Medicine, 725 North Wolfe Street, Baltimore, MD 21205, USA.

*These authors contributed equally to this report.
†To whom correspondence should be addressed. E-mail: david_ginty@qmail.bs.jhu.edu